Detection of New Dissociative Electron Attachment Channels in NO

O. J. Orient and A. Chutjian
Jet Propulsion Laboratory, California Institute of Technology, Pasadena, California 91109
(Received 21 February 1995)

Three dissociative electron attachment channels have been detected and identified in NO via measurement of the $O^-(^2P)$ fragment energy. In addition to the known $N(^2D°) + O^-(^2P)$ channel, two new channels $N(^4S°) + O^-(^2P)$ and $N(^2P°) + O^-(^2P)$ were detected. Cross sections for each of the channels are reported by normalizing the scattering intensities to previously measured total cross sections. The experimental approach uses solenoidal magnetic confinement of the electrons and ions, and trochoidal energy analysis of the low-energy ions.

PACS numbers: 34.80.Gs, 82.80.Fk

Reported herein are ion energies and dissociative attachment (DA) cross sections for three channels producing N + O^- fragments from NO. The reaction channels are

$$e + NO(X^2\Pi_r) \rightarrow N(^4S°) + O^-(^2P) \quad (1a)$$

$$\rightarrow N(^2D°) + O^-(^2P) \quad (1b)$$

$$\rightarrow N(^2P°) + O^-(^2P). \quad (1c)$$

Prior to this work, only reaction (1c) had been identified [1].

Using the approach of Refs. [1] and [2], one may relate the most probable ion energy E_i released in processes (1a)–(1c) to the incident electron energy E_e by

$$E_i = \frac{\mu}{m_0}[E_e - (D_0^\circ - A + E^*)], \quad (2)$$

where μ is the reduced mass of NO, m_0 the mass of oxygen, D_0° is dissociation energy of NO (6.497 eV [3]), A its electron affinity (1.461 eV [4]), and E^* the energy intervals in atomic nitrogen which are 2.384 eV for the $N(^4S°\text{-}^2D°)$ separation and 3.576 eV for the $N(^4S°\text{-}^2P°)$ separation [5]. Through knowledge of the electron energy E_e and the outgoing ion energy E_i, one may identify the reaction channels in (1a)–(1c) via Eq. (2) or through more detailed dynamics (see below).

The apparatus used to form O^- and measure the ion energies and intensities has also been used to generate intense beams of ground-state $O(^3P)$ atoms in fast atom-molecule and atom-surface collisions studies [6]. A schematic diagram of the configuration used in the present work is shown in Fig. 1. The entire experiment is carried out in a uniform, solenoidal, 6 T magnetic field. Briefly, electrons (e) are extracted from a hot, spiral-wound tungsten filament (F), accelerated to the range 7.5–10.0 eV, and attached to a beam of NO effusing from a 1 mm diam hypodermic needle. The emerging O^- ions (with kinetic energies in the range 0.2–4 eV) and parent-beam electrons are deflected in a trochoidal monochromator (TM) of length 7.87 cm. The electrons and slower ions are deflected by about 2 and 43 mm, respectively. Electrons are collected in a Faraday cup (FC_e). The spiraling ions are transported through two slits and a shielded cage, and detected in an analog mode in a second Faraday cup (FC_i). The ion current S is then digitized and stored in a personal computer as a function of the TM electric field. Typical electron and ion currents are 10^{-5} and 10^{-9} A, respectively. Pressures during operation near the NO beam are 6.7×10^{-5} Pa (5×10^{-7} Torr) and at the detector FC_i 6.7×10^{-7} Pa (5×10^{-9} Torr). This is a new experimental approach which can be used to study a variety of electron attachment and ionization processes in atoms and molecules. Use at lower solenoidal magnetic fields and with various TM geometries is possible.

Energy spectra and relative attachment intensities of the O^- ions resulting from DA to NO are shown in Fig. 2 at three electron energies E_e. Each of the three features was deconvoluted from the measured spectrum. The total relative attachment intensity $I(E_e, E_i)$ measured in FC_i is given by the sum over the final $N(S, D, P)$ states,

$$I(E_e, E_i) = I_S(E_e, E_i) + I_D(E_e, E_i) + I_P(E_e, E_i). \quad (3)$$

The three components are deconvoluted assuming a Gaussian line shape,

$$I_{S,D,P}(E_e, E_i) = I^0_{S,D,P} \exp\{-[2(E_i - E^0_{S,D,P}/W_{S,D,P})]^2 \ln 2\}, \quad (4)$$

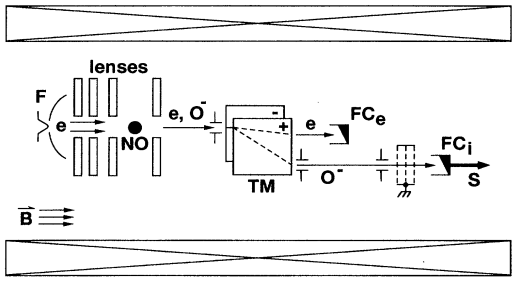

FIG. 1. Schematic diagram (not to scale) of the magnetically confined trochoidal system. Electrons (e) from a filament (F) attach in the energy range 7.5–10.0 eV to a beam of NO to form $O^-(P)$ ions. The ions and parent electrons are separated by the trochoidal monochromator (TM), and the resulting energy-analyzed ion signal S is detected at FC_i in an analog mode. Length of the solenoidal magnet is 1 m.

0031-9007/95/74(25)/5017(3)$06.00

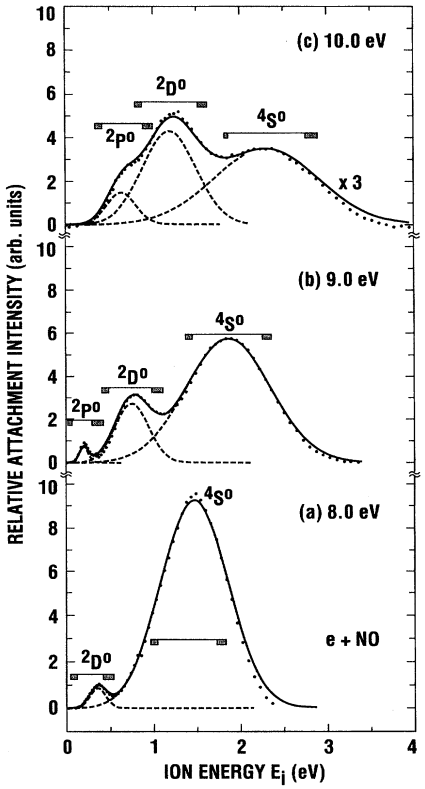

FIG. 2. Energy spectra of the channels $O^-(^2P)$ + $N(^2P°, ^2D°, ^4S°)$ in DA to NO at the indicated electron energies of (a) 8 eV, (b) 9 eV, and (c) 10 eV. Dashed lines are results of unfolding; the solid line is the calculated sum intensity to be compared with data (•). Lines above each feature represent the range of ion energies for the range $\theta(0, \pi)$, including contribution from a ±0.2 eV electron beam width [shaded areas, Eq. (5)].

where $E^0_{S,D,P}$ is the peak energy of the transition, $I^0_{S,D,P}$ the peak intensity, and $W_{S,D,P}$ the full width at half maximum (FWHM). Results of the unfolding are shown in Fig. 2 (dashed lines) for an average width $\overline{W}$ given by $W_{S,D,P}/E_i = \overline{W}/E_i = 0.61$.

To treat the dynamics of the DA process, we regard the N and O^- fragments as emerging from a case where the center-of-mass (CM) energy is zero. The O^- fragment has a laboratory (LAB) energy given by [7]

$$\Delta E_0 = \frac{\mu}{m_0}\Delta E_{\mathrm{CM}} + \cos\theta\sqrt{\frac{4\mu}{M}E_0\Delta E_{\mathrm{CM}}}. \qquad (5)$$

Here, M is the total mass of NO, E_e the incident NO energy, and θ the CM angle of the departing O^- ion relative to the CM velocity along the incident NO direction. ΔE_{CM} is the total CM energy available for fragment translational energy, which is also the factor in brackets in Eq. (2).

One may use Eq. (5) to calculate the LAB energy of O^- and compare it to measurements. Shown in Fig. 2 above each feature are the ranges of calculated energies possible in the collision [Eq. (5)], with θ taken in the entire CM interval $(0, \pi)$. It is useful to point out an important feature of the present experimental configuration relative to that of Refs. [1] and [2]. The O^- ions produced at the NO beam (Fig. 1) are immediately confined by the large (6 T) solenoidal magnetic intensity. Trajectory calculations ignoring space charge show that ions having energies of the order of 1 eV are directed along the solenoidal **B** field, including those ions ejected at $\theta = 0°$ (along the NO beam). Ions directed upstream (towards F) are reflected towards TM by a mirroring potential at the cathode. In contrast, extraction voltages in Refs. [1] and [2] had to be a compromise between the best ion collection possible with a flat-plate collector and preservation of energy resolution of the electron beam (the electron beam was magnetically confined, but the ions were not).

In addition, the available CM energy will depend on the energy width of the electron beam [width of E_e in Eq. (2)]. A spiral-wound, 0.016 in. diam tungsten wire was used as the electron emitter. Because of the large emitter surface area, low filament currents (hence, low filament temperature) were required. We estimate the filament temperature to be about 2000 K, corresponding to an electron-energy width of about $2.5kT = 0.4$ eV (FWHM). Using this value, one obtains a slightly larger range of possible O^- energies, given by the shaded additions in Fig. 2.

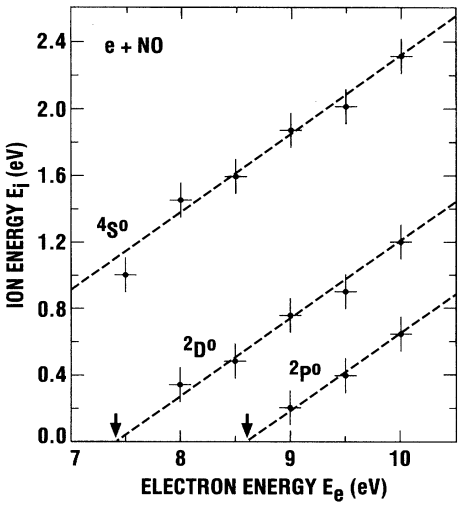

FIG. 3. Unfolded peak intensities of the channels $O^-(^2P)$ + $N(^2P°, ^2D°, ^4S°)$ in DA to NO as a function of attaching electron energy E_e. Straight lines are drawn with the theoretical kinematic slope of $\mu/m_0 = 14/30$. Threshold energies are 8.611 eV ($^2P°$), 7.419 eV ($^2D°$), and 5.035 eV ($^4S°$, not indicated).

Not included in this estimate of the energy range are two additional effects: (a) Anisotropic scattering intensity in the range $\theta(0, \pi)$ due to different angular differential cross sections [DCS(θ)] for each energy and transition. We have assumed a constant DCS(θ), and the use of the actual DCS(θ) would tend to narrow the distributions by limiting the effect to the peak of the DCS(θ). (b) Energy broadening of the TM (Fig. 1). From simple considerations (the length and spacing of the plates, aperture diameters at the entrance and exit), an energy broadening $W_{\mathrm{TM}}/E_i = 0.39$ is calculated. This effect would broaden all peaks, depending on their location in E_i, and is almost certainly responsible for the tailing in the O^- distributions (Fig. 2).

To demonstrate in an alternate way the correct energy dependence of the transitions, plotted in Fig. 3 are the energies of the peak unfolded intensities as a function of E_e. The dashed line through each of the data points represents the theoretical slope $\mu/m_0 = 14/30$, consistent with Eq. (2).

Finally, one may relate the DA cross section for each channel $\sigma_{S,D,P}(E_e)$ to the total attachment cross section $\sigma_T(E_e)$ by

$$\sigma_T(E_e) = C\left[\int_0^\infty I_S(E_e, E_i)dE_i + \int_0^\infty I_D(E_e, E_i)dE_i + \int_0^\infty I_P(E_e, E_i)dE_i\right]. \quad (6)$$

Here, C is a normalization constant which relates the total-collected scattering intensities to the absolute total cross section $\sigma_T(E_e)$ reported in Ref. [8]. Calculation of C may be made from data at any electron energy. The channel cross sections are then given by

$$\sigma_S(E_e) = \frac{C\int_0^\infty I_S(E_e, E_i)dE_i}{\sigma_T(E_e)},$$

$$\sigma_D(E_e) = \frac{C\int_0^\infty I_D(E_e, E_i)dE_i}{\sigma_T(E_e)}, \quad (7)$$

$$\sigma_P(E_e) = \frac{C\int_0^\infty I_P(E_e, E_i)dE_i}{\sigma_T(E_e)}.$$

The normalization constant C may be calculated at each of the six energies at which $\sigma_T(E_e, E_i)$ were measured. These six values resulted in a value $C = (2.548 \pm 0.103) \times 10^{-16}$ cm^2 at the 1σ level of random error. DA cross sections for the three channels as a function of electron energy E_e are shown in Fig. 4 [9]. The errors indicated are the squared sum of the statistical error, unfolding error [assumption in Eq. (4)], and error in the underlying $\sigma_T(E_e)$.

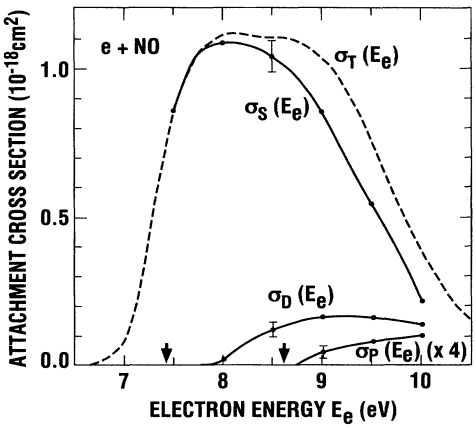

FIG. 4. Electron attachment cross sections $\sigma_S(E_e)$, $\sigma_P(E_e)$, and $\sigma_D(E_e)$ for the individual S, P, D channels normalized to the total cross sections $\sigma_T(E_e)$ of Ref. [8].

We thank Dr. E. Murad for his support. This work was carried out at the Jet Propulsion Laboratory, California Institute of Technology, and was sponsored by the Air Force Phillips Laboratory, Hanscom AFB, through agreement with the National Aeronautics and Space Administration.

[1] P. J. Chantry, Phys. Rev. **172**, 125 (1968).
[2] P. J. Chantry and G. J. Schulz, Phys. Rev. **156**, 134 (1967).
[3] K. P. Huber and G. Herzberg, *Molecular Spectra and Molecular Structure IV. Constants of Diatomic Molecules* (Van Nostrand Reinhold, New York, 1979), p. 466.
[4] H. Hotop and W. C. Lineberger, J. Phys. Chem. Ref. Data **14**, 731 (1985).
[5] S. Bashkin and J. O. Stoner, Jr., *Atomic Energy Levels and Grotrian Diagrams 1* (Elsevier, New York, 1975), p. 103.
[6] O. J. Orient, K. E. Martus, A. Chutjian, and E. Murad, Phys. Rev. A **45**, 2998 (1992).
[7] F. Brouillard and W. Claeys, in *Physics of Ion-Ion and Electron-Ion Collisions*, edited by F. Brouillard and J. Wm. McGowan (Plenum, New York, 1983), p. 415.
[8] D. Rapp and D. D. Briglia, J. Chem. Phys. **43**, 1480 (1965).
[9] It is interesting to point out recent measurements [C. T. Kuo, J. L. Hardwick, and J. T. Moseley, J. Chem. Phys. **101**, 11 084 (1994)] of the DA cross section to the excited $A^2\Sigma^+$ state of NO at 0.5 eV electron energy. This value of 2.0×10^{-15} cm^2 is a factor of 1800 greater than that for DA to the ground state, $\sigma_T(E_e) = 1.11 \times 10^{-18}$ cm^2. The increase is due to a core-excited Feshbach resonance near the A state.